

Have tropical cyclones been feeding more extreme rainfall?

K.-M. Lau,¹ Y. P. Zhou,² and H.-T. Wu³

Received 14 February 2008; revised 23 September 2008; accepted 9 October 2008; published 13 December 2008.

[1] We have conducted a study of the relationship between tropical cyclone (TC) and extreme rain events using GPCP and TRMM rainfall data, and storm track data for July through November (JASON) in the North Atlantic (NAT) and the western North Pacific (WNP). Extreme rain events are defined in terms of percentile rainrate, and TC-rain by rainfall associated with a named TC. Results show that climatologically, 8% of rain events and 17% of the total rain amount in NAT are accounted by TCs, compared to 9% of rain events, and 21% of rain amount in WNP. The fractional contribution of accumulated TC-rain to total rain, Ω , increases nearly linearly as a function of rainrate. Extending the analyses using GPCP pentad data for 1979–2005, and for the post-SSM/I period (1988–2005), we find that while there is no significant trend in the total JASON rainfall over NAT or WNP, there is a positive significant trend in heavy rain over both basins for the 1979–2005 period, but not for the post-SSM/I period. Trend analyses of Ω for both periods indicate that TCs have been feeding increasingly more to rainfall extremes in NAT, where the expansion of the warm pool area can explain slightly more than 50% of the change in observed trend in total TC rainfall. In WNP, trend signals for Ω are mixed, and the long-term relationship between TC rain and warm pool area is strongly influenced by interannual and interdecadal variability.

Citation: Lau, K.-M., Y. P. Zhou, and H.-T. Wu (2008), Have tropical cyclones been feeding more extreme rainfall?, *J. Geophys. Res.*, 113, D23113, doi:10.1029/2008JD009963.

1. Introduction

[2] Recent studies have indicated that a warming trend in sea surface temperature (SST) may be responsible for increasing hurricane intensity in the past several decades [Emanuel, 2005; Webster *et al.*, 2005]. Climate models have predicted increases in both storm intensity and near-storm precipitation rates in a warming environment induced by increasing greenhouse gases [Knutson and Tuleya, 2004]. However it is well known that hurricane activity is influenced by a multitude of environmental factors including not only SST [Shapiro, 1982; Shapiro and Goldenberg, 1998; Saunders and Harris, 1997] but also sea-level pressure [Landsea *et al.*, 1998; Gray, 1984; Knaff, 1997], troposphere moisture [Landsea *et al.*, 1998], vertical wind shear, and stratospheric quasi-biennial oscillation [Gray, 1968, 1984; Goldenberg and Shapiro, 1996; Shapiro, 1989; Shapiro and Goldenberg, 1998; Landsea *et al.*, 1998]. These factors may be further influenced by dominant weather and climate variabilities such as El Niño, multi-decadal oscillation, African easterly wave, and West African Sahel rainfall [Gray, 1990; Goldenberg and

Shapiro, 1996; Goldenberg *et al.*, 2001; Landsea and Gray, 1992; Landsea, 1993; Landsea *et al.*, 1994].

[3] Similarly, interannual variability of typhoon activity over the western North Pacific is strongly regulated by the El Niño-Southern Oscillation through its influence on the monsoon trough, low-level relative vorticity, vertical wind shear and moist static energy [Chan and Liu, 2004; Wang and Chan, 2002]. Because of the large interannual and interdecadal variabilities of factors that influence hurricane/typhoon activity, and inherent uncertainties in long-term hurricane records, identifying a linkage between hurricane/typhoon (hereafter collectively referred to as tropical cyclone, TC) and global warming is a very challenging task [Henderson-Sellers *et al.*, 1998; Trenberth, 2005; Pielke *et al.*, 2005; Shepherd and Knutson, 2006].

[4] On the other hand, studies have shown that precipitation characteristics are more likely subject to climate change than total precipitation amount [Trenberth *et al.*, 2003]. Lau and Wu [2007] analyzed 25 years of satellite rainfall data and found a significant shift in the rainfall distribution that indicates positive trends in extreme heavy and light rains, and a negative trend in moderate rain in the tropics. Studies also show that precipitation mostly in the upper percentile of the distribution over the United State has increased in recent decades and that the portion of total precipitation derived from extreme and heavy events increased significantly [Karl and Knight, 1998; Groisman *et al.*, 2004]. Extreme rain events can arise from a variety of severe weather systems such as squall lines, meso-scale convective complexes, tropical supercloud clusters, TCs

¹Laboratory for Atmospheres, NASA, Goddard Space Flight Center, Greenbelt, Maryland, USA.

²Goddard Earth Sciences and Technology Center, University of Maryland Baltimore County, Catonsville, Maryland, USA.

³Science Systems and Applications, Inc., Lanham, Maryland, USA.

and others. Given the increasing evidence on the connection between extreme weather events and climate change [Trenberth *et al.*, 2007], it may be instructive to understand the linkage between TC activity and climate change through the perspective of extreme rain events. Recent studies have shown that TCs may have contributed to increase in extreme heavy rainfall in many different regions of the world, in particular along the coastal regions of South China and southeastern United States [Wu *et al.*, 2007; Shepherd *et al.*, 2007]. The questions we address in this paper are: What are the relationships between extreme rain events and TC activity? Can we detect long-term trends in current multi-decadal satellite rainfall data? If so, would it be possible to infer a linkage between TC activity and SST through statistics of rainfall extremes? Past studies of trends of intense TCs may have suffered from uncertainties stemming from changes in the definition of TC intensity by different operational centers, based on sustained maximum wind or subjective satellite imagery interpretation [Velden *et al.*, 2006; Landsea *et al.*, 2006]. Up to now, there have been very few observational studies linking possible trends in TC to tropical rainfall [Groisman *et al.*, 2004]. In this paper, we use percentile ranked rain rate from satellite rainfall data, to examine possible trends in TC contribution to extreme rainfall statistics.

2. Data and Methodology

[5] Data used in this study include the pentad rainfall from the Global Precipitation Climatology Project (GPCP) for 1979–2005 [Xie *et al.*, 2003], the 3-hourly Tropical Rainfall Measurement Mission (TRMM) Multi-satellite Precipitation Analysis (TMPA) data for 1998–2005 [Huffman *et al.*, 2007], the 6-hourly best storm track data for North Atlantic (NAT) [Jarvinen *et al.*, 1984] and western North Pacific (WNP) [Chu *et al.*, 2002] for 1979–2005 from the National Hurricane Center and the Joint Typhoon Warning Center, respectively, with a correction of wind speed [Emanuel, 2005]. The Hadley Center monthly data (1979–2005) is used for the SST analysis [Rayner *et al.*, 2003]. The 3-hourly TMPA data is used to generate daily gridded precipitation data. The spatial resolution is 2.5° latitude \times 2.5° longitude for GPCP, $0.25^\circ \times 0.25^\circ$ for TRMM, and $1^\circ \times 1^\circ$ for SST. The analyses in this study are based on a large oceanic domain (20°W – 90°W , 10°N – 40°N) over NAT, and a domain with comparable size (120°E – 180°E , 10°N – 40°N) over WNP during the major TC season, July through November (JASON). Following the approach described in Lau and Wu [2007], we construct the probability distribution function (PDF) and cumulative PDF (CPDF) of rain amount and rain frequency, with the data binned at the interval of 1 mm/day. Rainfall extremes are defined with respect to ranked rain rates, as top 20% (T20), top 10% (T10), and top 5% (T5) extreme rain, from the CPDFs of rain amount in each ocean domain. The results to be shown are independent of the exact percentile ranks, which are only chosen as representative markers to quantify the extreme rain events. Using this notation, the total rain can be labeled as T100.

[6] In order to examine the TC contributions to the total rain and to each rainfall category, we calculate the TC-related rainfall using the 6-hourly storm track data for both

NAT and WNP. Following Larson *et al.* [2005] and Rodgers *et al.* [2000, 2001], we define TC-rain as rain that falls within an area of 500 km radius, from the center of the TC, i.e., assuming that rainfall occurs within the 500 km of storm center is all associated with the TC during the same day the TC occurs. This procedure is applied to the TRMM daily data. Because of GPCP's coarse spatial and temporal resolutions, we define the pentad rain as TC-rain if a TC passes through during anytime of the pentad within 500 km of the grid box. If the pentad rain meets the criteria of extreme rain, it is further defined as TC-related extreme rainfall. The GPCP TC-rain defined in this way is only a crude approximation to actual TC-rain, because it may overestimate the direct TC contribution, since other forms of rain may have contributed to the total rainfall in the pentad. On the other hand, it may under-estimate TC-rain contribution in extreme rain categories, because some heavy TC-rain may not be counted in the extreme rainfall if the corresponding GPCP pentad is not qualified as an extreme event due to GPCP's coarse space-time resolution. The consistency between the TRMM-defined and GPCP-defined rainfall extremes and TC-rain statistics are examined in section 3.1.

[7] The GPCP pentad data used in the study is a merged product that combines available surface rain gauge and operational satellite rainfall estimates to provide a state-of-the-art, multi-decadal global data set for climate studies [Adler *et al.*, 2003; Xie *et al.*, 2003]. In view of the possible data inhomogeneity by changes in satellite rainfall algorithms, especially the shift from mainly infrared-based before 1988, to addition of microwave-based, Special Sensor Microwave/Imager (SSM/I) algorithms after 1988, GPCP has been designed to preserve temporal homogeneity maximally. For example, it did not incorporate the more recent high resolution TRMM instrument. For consistency, only one SSM/I instrument is selected at a time, from satellites with early equatorial crossing time (F8, F11, F13) (Ferraro, personal communication). The monthly GPCP has been cross-calibrated before 1988 (pre-SSM/I) with later period (post-SSM/I) based on an overlapping period to minimize the systematic bias [Adler *et al.*, 2003]. The pentad GPCP is matched to the monthly GPCP in that the pentad approximately sums to the monthly estimate. However this calibration is not likely to eliminate all the biases with respect to the inhomogeneity due to the inclusion of SSM/I since 1988. Hence results incorporating GPCP data for both the pre- and post-SSM/I period should be treated with extreme caution. This study should be considered as a “best-effort” attempt at exploring extreme rainfall trend signals, and their possible relationship with SST, using the only available multi-decadal satellite rainfall data. In the following analyses, we will discuss the trends derived from the entire 27-year period (1979–2005) and compare with those derived from the 18-year post-SSM/I period (1988–2005) only, in order to get a better assessment of the real climate trend, as well as possible data limitation.

3. Results

3.1. Extreme Rain and TC-Rain Climatology

[8] In this section, we discuss the basic statistics of extreme rainfall and TC-related rainfall (TC-rain) based

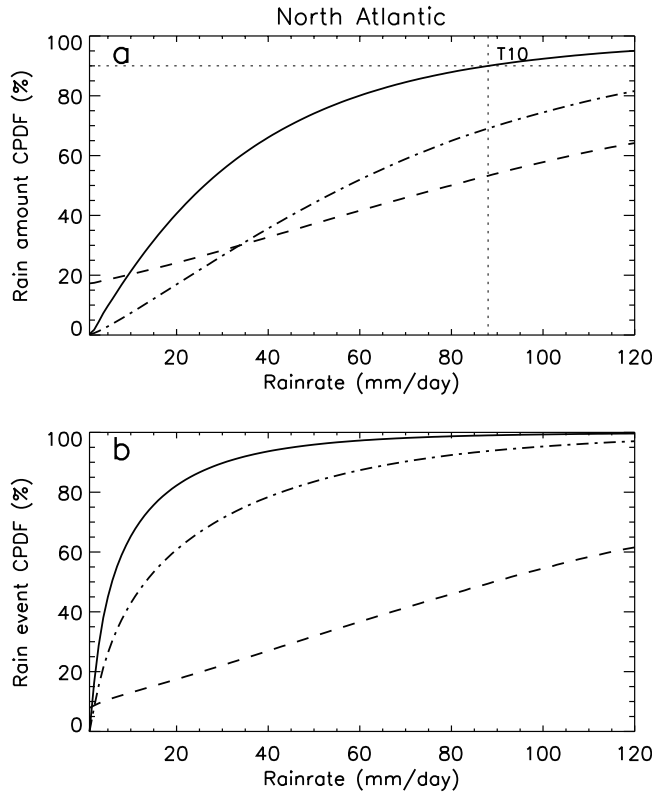


Figure 1. Cumulative PDF of daily rainfall (solid line), and TC-rain (dash-dot line), from TRMM data for NAT during JASON, 1998–2005, for (a) rainfall amount and (b) frequency of occurrence. The dashed line in (a) shows the fractional TC-rain to total rain amount, Ω , and in (b) the fractional TC events to total rain events.

on the daily TRMM data, for NAT and WNP respectively, to provide background for understanding the main results shown in sections 3.2 and 3.3. We also examine the consistency of TRMM-derived and the GPCP-derived rain statistics for the overlapping periods (1998–2005) to ensure that GPCP pentad data are good for trend analysis for the extended period (1979–2005). To facilitate the analysis, we define the following relationships:

$$\begin{aligned} \mathbf{AR}_{TC}(r) &= \Omega(r)\mathbf{AR}(r), \\ \mathbf{AR}_{TC}(r) &\equiv \int_r^\infty \mathbf{R}_{TC}(r)dr, \text{ and } \mathbf{AR}(r) \equiv \int_r^\infty \mathbf{R}(r)dr, \end{aligned} \quad (1)$$

where $\mathbf{R}_{TC}(\mathbf{r})$ is the TC-rain amount, and $\mathbf{R}(\mathbf{r})$, the total rain amount for a given rainrate, \mathbf{r} ; $\mathbf{AR}_{TC}(\mathbf{r})$ and $\mathbf{AR}(\mathbf{r})$, the

Table 1a. TC Related Extreme Event Rainfall Statistics Based on TRMM Data for NAT (90°W–20°W, 10°N–40°N) During JASON 1998–2005^a

	T5	T10	T20	Total
TRMM-threshold (mm/day)	119.0	88.0	60.0	—
Ω -event (%)	61.3	49.4	36.7	7.9
Ω -amount (%)	63.9	53.2	41.6	17.3

^aStatistics are area weighted. Ω -event and Ω -amount indicate the fractional contributions of cumulative TC to total rain for rain event and rain amount (see text for definition), respectively.

Table 1b. Same as in Table 1a, Except for WNP (120°E–180°E, 10°N–40°N)

	T5	T10	T20	Total
TRMM-threshold (mm/day)	136.0	101.0	69.0	—
Ω -events (%)	61.5	53.2	42.5	9.0
Ω -amount (%)	64.2	56.7	46.9	20.6

accumulated TC-rain and accumulated total rain with rainrate greater than \mathbf{r} ; $\Omega(\mathbf{r})$ is a scaling factor representing the fractional contribution of accumulated TC-rain to total rain. Note that from (1), the accumulated total rain, and total TC-rain is denoted by $\mathbf{AR}(0)$ and $\mathbf{AR}_{TC}(0)$ respectively.

[9] Figure 1a shows the CPDFs associated with total rain ($1-\mathbf{AR}(\mathbf{r})/\mathbf{AR}(0)$), TC rain ($1-\mathbf{AR}_{TC}(\mathbf{r})/\mathbf{AR}_{TC}(0)$), and the ratio $\Omega(\mathbf{r})$ in NAT. Similar CPDFs for the rain event have been constructed (Figure 1b), with the rainfall amount replaced by the frequency of occurrence (FOC) of rain events. For low rain rates, the CPDF of total rain increases more rapidly than that of TC rain. For high rain rates, the reverse holds. These indicate that TC contributes more to heavy rain events than to light rain events. Interestingly, the percentage contribution of \mathbf{AR}_{TC} to \mathbf{AR} , as represented by the scaling factor Ω , increases approximately linearly as a function of rain rate. As shown by the intercepts of Ω at the ordinate, i.e., $\Omega(0)$ in Figure 1a, and also in Table 1, the total TC-rain accounts for a significant portion (17.3%) of the total rain amount, but occurs rather infrequently, accounting for only 7.9% of the FOC (as shown by Figure 1b). For extreme rain, for example T10, 49% of rain events, and 53% of rain amount are accounted for by TC-rain for NAT. These results are consistent with *Shepherd et al.* [2007] who found that TCs, particularly stronger storms (>Cat. 3), contributed most to extreme rainfall (for example, defined as Wet Millimeter Days in their study) in Gulf of Mexico and East U.S. coastal areas. The percentage of TC contribution to total rain is slightly higher in this study as compared to *Shepherd et al.* [2007] and *Rodgers et al.* [2001], possibly due to differences in domain sizes, and study periods. For WNP, the CPDFs (not shown) are similar, including the nearly linear increase in Ω with rainrate. Our estimates of WNP TC-rainfall are also comparable to those of *Wu et al.* [2007] and *Rodgers et al.* [2000]. The key CPDF statistics for NAT and WNP are shown in Tables 1a and 1b. Comparing the Ω factors in the two domains, the TCs in WNP appear to produce more intense rain than in NAT, accounting for 9.0% of rain occurrence, but 20.6% of the total rain amount. The higher rainfall intensity for WNP TCs is also reflected in the higher rainfall thresholds in all three extreme rain categories (T5, T10 and T20). At T10 for WNP, TC-rain accounts for 53% rain events and 57% rain amount. At T5, the corresponding ratios are 62% and 64%. The Ω factors appear to approach a common value ($\sim 65\%$ for T5 rain amount) for highly extreme events for both domains. This means that even at

Table 2a. Same as in Table 1a for NAT, Except for Using GPCP Pentad Data

	T5	T10	T20	Total
GPCP-threshold (mm/day)	23.0	18.0	13.0	—
Ω -event (%)	54.6	45.4	35.8	9.7
Ω -amount (%)	55.9	47.8	39.3	19.6

Table 2b. Same as in Table 1b for WNP, Except for Using GPCP Pentad Data

	T5	T10	T20	Total
GPCP-threshold (mm/day)	33.0	26.0	19.0	—
Ω -events (%)	77.1	68.4	55.7	12.2
Ω -amount (%)	78.3	70.3	59.3	27.2

such highly extreme rain events, non-TC-rain can still contribute no less than 30% of the rain amount.

[10] Similar CPDFs are constructed from GPCP data for the overlapping period of the two data sets (1998–2005). For

comparison, the statistics for GPCP-defined extreme events are shown in Tables 2a and 2b for NAT, and WNP respectively. Since the GPCP pentad rainfall has lower spatial and temporal resolutions compared to TRMM, TC-rain can only be defined for the entire pentad, i.e., counting all rainfall within a pentad, if a TC passes over a given location during anytime of the pentad. Comparing Tables 2a and 2b with Table 1, it is clear that even though the thresholds for the GPCP extreme events are considerably lower relative to those for the daily TRMM data, the Ω factors are reasonably scale-invariant with respect to the extreme categories, with increasing TC contributions for heavier rains.

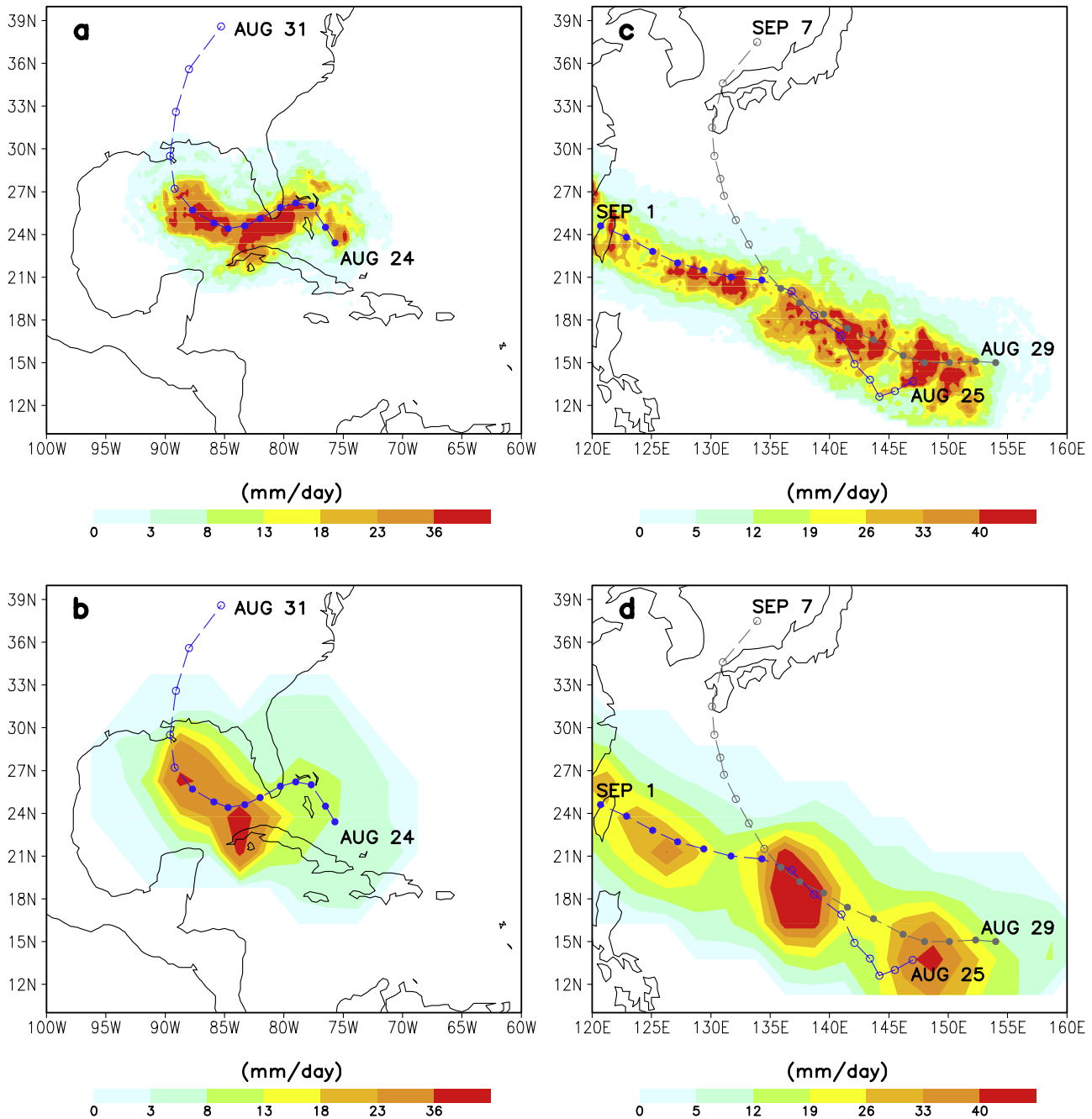


Figure 2. TC-rain from (a) TRMM and (b) GPCP during 24–28 August 2005 overlay with best track of Hurricane Katrina. TC-rain from (c) TRMM and (d) GPCP during 29 August–2 September 2005 overlay with best tracks of Typhoons Nabi and Talim.

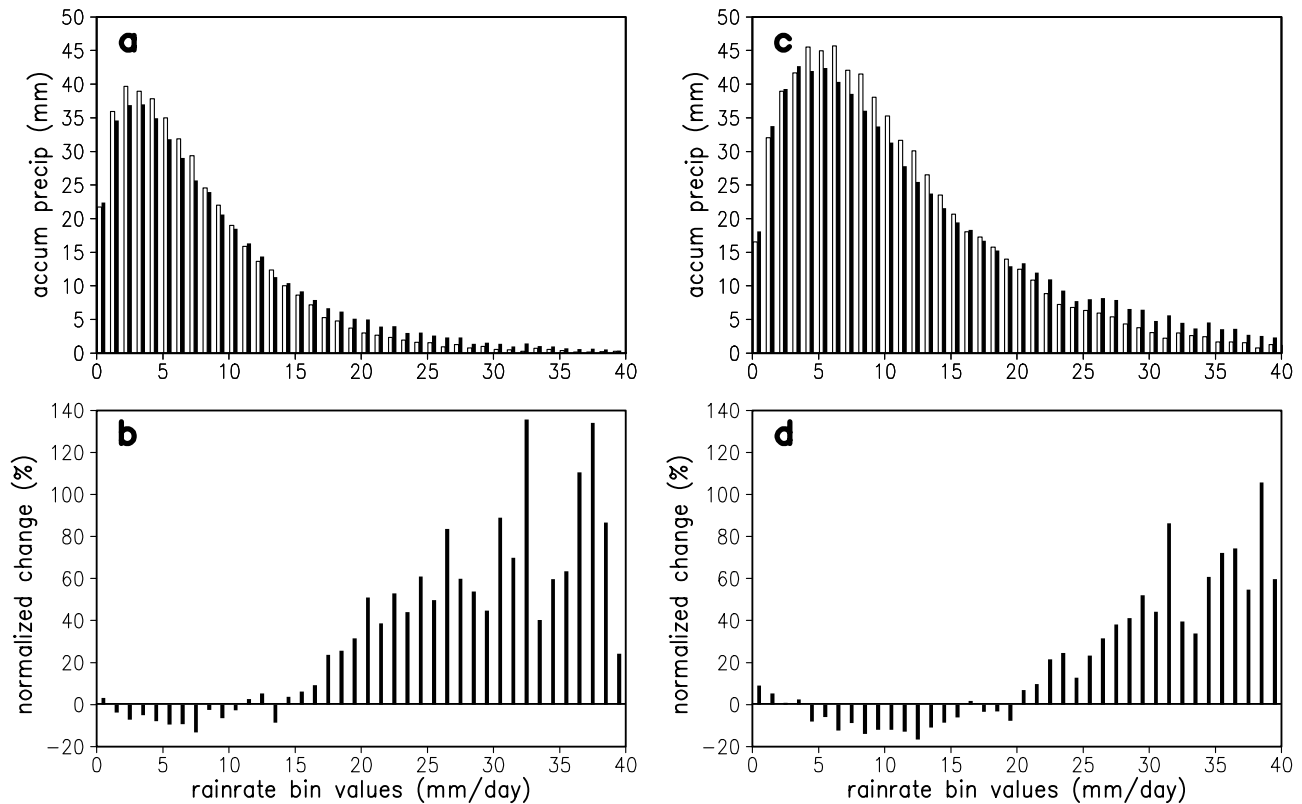


Figure 3. (a) The climatological PDF from GPCP for JASON accumulated rainfall amount at each rainfall bin (with 1 mm/day interval) of the first 13 years (1979–1991, outlined bar) and the latter 13 years (1993–2005, filled bar), and (b) shift in PDF shown as the difference between the rainfall PDF of the latter period (1993–2005) and the first period (1979–1991) normalized by the mean of these two periods, for NAT. (c) and (d), are the same as in (a) and (b), except for WNP.

[11] The spatial distributions of TC-rain (Figure 2) for a 5-day period during Hurricane Katrina (24–28 August 2005) and during Typhoons Talim and Nabi (29 August–2 September 2005) show good match in patterns and relative magnitudes between the GPCP-pentad rain and the 5-day rain constructed from the TRMM 3-hourly data, indicating that both data sets captured essentially the same TC-related rain systems. The distributions shown are typical of many other TC events we have examined. The above results provide some reassurance that the GPCP data can be used to study the relationship between extreme rain and TC-rain, for the extended period of the GPCP.

3.2. Trends in Rainfall Characteristics

[12] As demonstrated by previous studies, trends in rainfall characteristics may be manifested as shifts in the rainfall PDF. For the JASON season, a shift in the rainfall PDF from the first half (1979–1991) of the data record to the second half (1993–2005) is apparent for both domains (Figures 3a and 3c). The latter period shows increasing heavy rains, and decreasing moderate rains compared to the earlier. The strong signal in the extreme rain can be seen more clearly in the normalized deviation (difference between second and first periods divided by the mean of the two periods) for each rain bin (Figures 3b and 3d), which show clearly positive increments for heavy rain events with some very large (>50%) deviations for very

extreme events (T5 or above). The relative changes appear to be more pronounced in NAT compared to WNP. For NAT, positive trends are found for all heavy rain with rainrate greater than ~ 14 mm/day. For WNP, the corresponding rainrate is ~ 20 mm/day. These values correspond to the rainrate thresholds for T20 rain category in the two ocean domains, respectively (see Tables 2a and 2b). A compensating negative trend in moderate-to-light rains (2 – 15 mm day $^{-1}$) is obvious in both domains.

[13] To examine the long-term variations of total rain, extreme rain, and associated TC contributions, we have constructed the time series of the seasonal (JASON) $\mathbf{AR}(\mathbf{r})$, and $\mathbf{AR}_{\text{TC}}(\mathbf{r})$ for the entire data period (1979–2005) for different threshold values of \mathbf{r} , that correspond to total rain ($\mathbf{r} = 0$), and to rainrate threshold (see Tables 2a and 2b) for extreme rain categories, T20, T10 and T5 respectively. Similarly, the accumulated FOC for the same rain categories have been computed. To suppress effects of El Niño Southern Oscillation (ENSO), and to highlight the long-term behavior, a 5-year running mean has been applied and the resulting time series are shown as thick solid or dashed lines in Figures 4 and 5. A vertical dash line is also drawn in each figure to mark the boundary between the pre-SSM/I and post-SSM/I periods. In the following, a time series is considered to possess a trend when its linear regression exceeds the 95% confidence level (c.l.), computed based on the R^2 statistical test [Wilks, 1995]. As shown in Figure 4a,

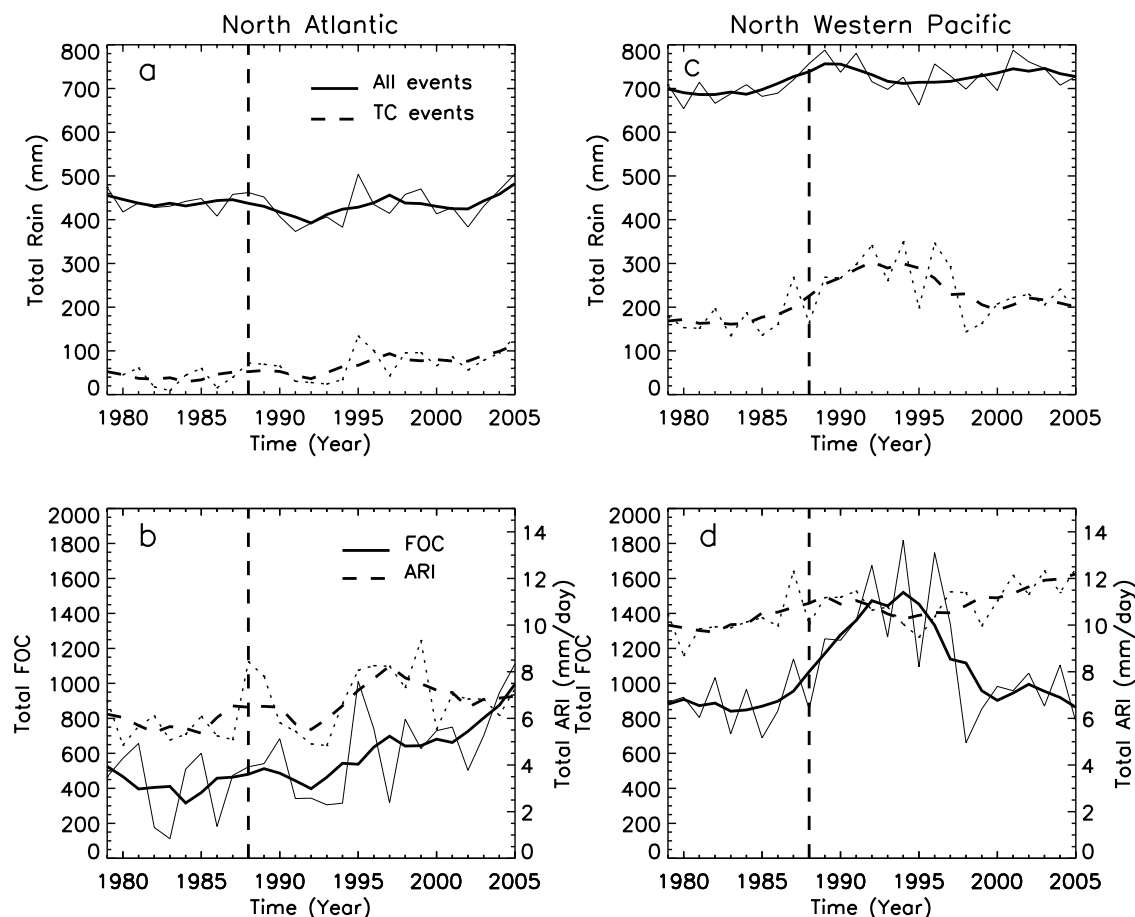


Figure 4. (a) Cumulative seasonal (JASON) GPCP total rainfall amount (solid line), $AR(0)$ and total TC-rain amount (dot line), $AR_{TC}(0)$ from 1979 to 2005. (b) Cumulative total TC frequency of occurrence (solid line) and TC accumulated rain intensity (dot line), ARI, for NAT. Thick lines show 5-year running mean. (c) and (d) are the same as in (a) and (b), except for WNP. Vertical dash lines separate the pre-SSM/I and post-SSM/I period.

in NAT, while the domain-average total GPCP rainfall, $AR(0)$ (labeled as all-event in Figure 4a), possesses no discernible trend, a trend exists in total TC-rain $AR_{TC}(0)$, especially for the post-SSM/I period. Figure 4b shows that the TC-rain possesses a significant trend in FOC, with strong signals coming from the post-SSM/I period. The accumulated TC rain intensity, ARI, defined as the AR_{TC} divided by FOC, shows a positive trend for the entire period, but only a weak indication of a trend for the post-SSM/I period. In contrast, in WNP, both the total rain, $AR(0)$, and total TC-rain amount, $AR_{TC}(0)$, show large decadal scale swings, and exhibit no obvious trends (Figure 4c). Notice also that $AR(0)$ and $AR_{TC}(0)$ in WNP are much larger than in NAT, with the TCs in the WNP producing more than double the rain amount in NAT. For WNP, TC-rain does not show a significant trend in FOC for the whole period. However the ARI shows a slight positive trend (Figure 4d) for the whole period, indicating a possible increase in rainfall intensity associated with TCs. As we will show later, the FOC seems to dominate the variation of TC contribution to extreme rain events. The results for trend analysis for extreme events are presented next.

[14] Since all three extreme rain categories have similar variability, only results for T10 are shown (Figure 5). For NAT, the T10 AR and AR_{TC} show large interannual and decadal variations with peaks in the late 1980s and mid-1990s and lows in the early 1980s (Figure 5a). Significant upward trends ($>99\%$ c.l.) are observed for both AR and AR_{TC} for the whole period. However the trends are weaker in the post-SSM/I period (see also the discussion for Table 3). The residual (figure omitted) computed as the difference between the two time series shows no clear long-term signal. Hence it can be inferred that the TCs are feeding dominantly to the variability and trend of AR for T10. Figure 5b shows that for T10, FOC also has a clear trend ($>99\%$ c.l.), similar to AR and AR_{TC} . There is a less pronounced trend in ARI for TC in this rain category (dotted line in Figure 5b). Both trends may have been contributed by suppressed activities during the pre-SSM/I period. For the post-SSM/I period, positive trends are still discernible, but much weaker. Regardless of the time period, the stronger trend in TC FOC, and its similarity in variations to AR imply that the observed trend in extreme rain amount (Figure 5a) is likely to be derived primarily from more TC events (either more TCs or TCs

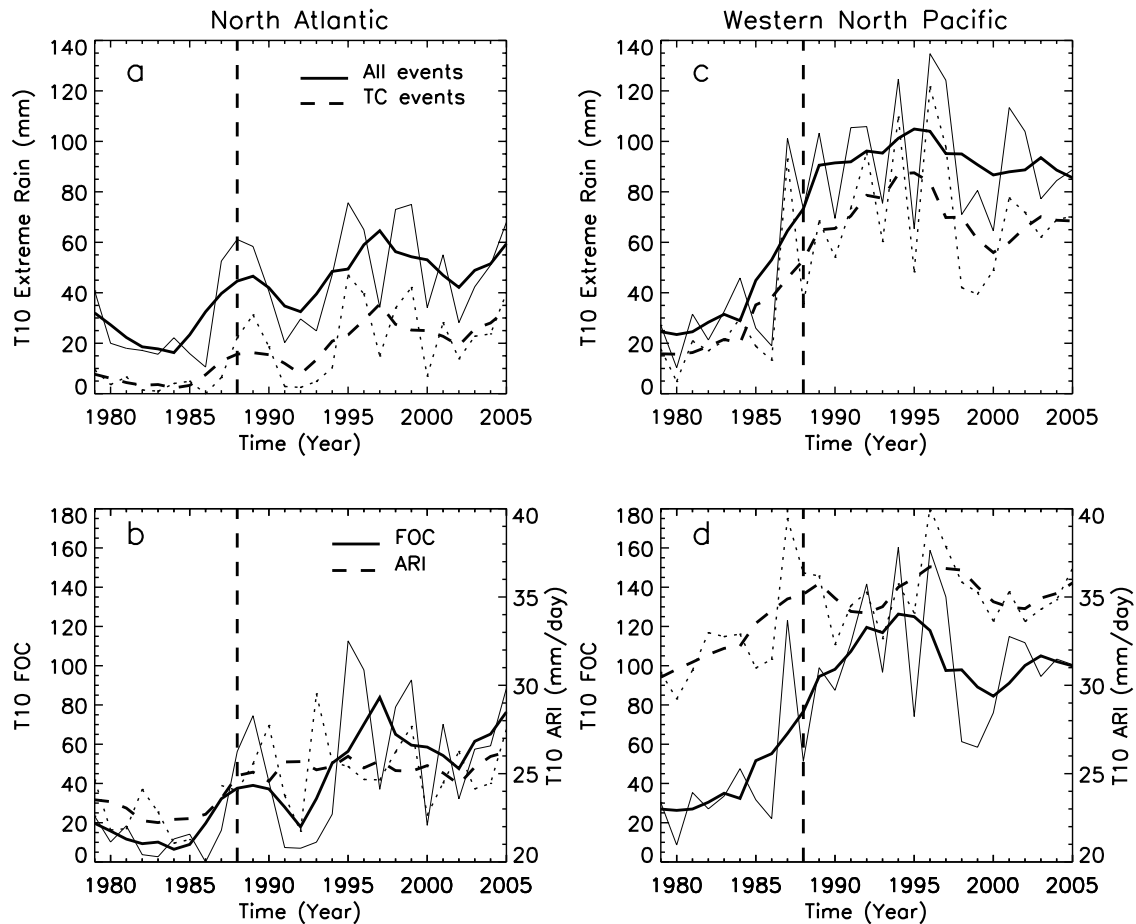


Figure 5. (a) Cumulative seasonal (JASON) GPCP rainfall amount (solid line), AR and TC-rain (dot line), AR_{TC} in T10 from 1979 to 2005. (b) Cumulative TC frequency of occurrence (solid line) and TC average rain intensity (dot line) in T10 for NAT. Thick lines show 5-year running mean. (c) and (d) are the same as in (a) and (b), except for WNP. Vertical dash lines separate the pre-SSM/I and post-SSM/I period.

with longer duration), and to a less degree from an increase in TC intensity.

[15] For WNP, large interannual and decadal variations dominate both AR and AR_{TC} for T10 (Figure 5c). The AR rises relatively steeply from 1984 to 1989, and stays nearly constant with a slight decline from 1995–2005. The AR_{TC} shows a similar rapid rise from the mid-1980s to the mid-1990s, followed by a more pronounced decline after 1995. The increasing number of WNP TCs from 1980 and the steep rise in mid-1980s to mid-1990s are reported in [Chan and Shi, 1996] and [Chan and Liu, 2004], respectively. As a result, although both AR and AR_{TC} show significant linear trends for the entire period, much of the signal may be attributed to the pre-SSM/I period, possibly as part of a decadal-scale variation, and/or due to inhomogeneity between the pre- and post-SSM/I data (see further discussion for Table 3). The closeness of the two time series suggests that TCs contribute strongly to the variability and trend of the extreme rain event in WNP. The FOC time series for T10_{TC} events (Figure 5d) shows long-term variations similar to the T10 rain amount (solid curve in Figure 5c), suggesting that variations in extreme rain may be due to TC events. The TC ARI for T10 in WNP also shows an apparent positive trend, but

with much of the signal coming from the pre-SSM/I period.

3.3. Relationships With SST

[16] Previous studies have noted that NAT and WNP have been warming at a moderate rate of approximately 0.5°C or less from 1980 through 2005 [e.g., Webster *et al.*, 2005]. Because of the strong control by surface evaporation on TC intensity [Emanuel, 1987], and that TCs are seldom formed when SST is below 26°C , it has been suggested that TC activity may be sensitive to the area of the warm pool [Wang *et al.*, 2006]. This suggestion has yet to be confirmed by climate models because of the complex factors affecting tropical cyclogenesis. For example, the NCAR CSM1 predicts that the threshold SST for tropical deep convection in a warmer climate may also increase hence expanding the 26°C isotherm is likely to have little effect on areal extent of cyclogenesis [Dutton *et al.*, 2000], while others [Wang *et al.*, 2008] found reduced tropospheric vertical wind shear in the main hurricane development region, and increased moist static instability of troposphere in the presence of a larger north Atlantic warm pool, both of which favor the intensification of tropical storms into major hurricanes. Here we examine the relationship of SST warm pool area with TC

Table 3. Linear Regression Expressed as Change per Decade of July–November TC Rain Amount and its Fractional Contribution (Ω) in Different Rain Categories Based on the 1979–2005 and 1988–2005 Data, Respectively, for (a) NAT, and (b) WNP^a

a. North Atlantic	1979–2005	1988–2005
T100-TC	*24.9 mm	29.2 mm
T20-TC	*14.8 mm	11.3 mm
T10-TC	*11.1 mm	7.3 mm
T5-TC	*7.4 mm	4.8 mm
Ω -T20 (%)	*12%	<u>11%</u>
Ω -T10 (%)	*15%	<u>13%</u>
Ω -T5 (%)	*18%	<u>15%</u>
warm pool area	*14%	*22%
b. North Western Pacific	1979–2005	1988–2005
T100-TC	23.6 mm	–43.2 mm
T20-TC	*26.0 mm	–6.8 mm
T10-TC	*23.4 mm	0.8 mm
T5-TC	*15.1 mm	0.8 mm
Ω -T20 (%)	3%	–1%
Ω -T10 (%)	4%	3%
Ω -T5 (%)	4%	3%
warm pool area	*6%	*9%

^aAlso shown is the change in the ratio of warm pool (SST > 28°C) area to total area (last row). Values exceeding 95% significance level are highlighted in bold. Asterisks indicate greater than 99% significance. Values with marginal (~90%) significance level are underlined.

related rainfall and extreme rain. The warming signals in NAT and WNP are most pronounced at the higher SSTs as evidenced in the PDF of SST constructed using a 0.5°C bin for two ocean basins in JASON for the first (pre-1992) and the second half (post-1992) periods (Figure 6). In NAT (Figures 6a and 6b) there is a clear signal of increase in FOC of SST > 28–29°C, and decreased occurrence of cooler SST (<28°C). Similar shifts in the SST PDF can be found in WNP (Figures 6c and 6d). If we define the size of the warm pool as area with SST > 28°C, the PDF shift translates into an increase in total warm pool area of approximately 14% per-decade in NAT, and only 6% per-decade in WNP respectively for the entire period (Table 3).

[17] Figure 7 shows the relationship between the warm pool area and the fractional contribution of TC-rain to total rain, i.e., the Ω factor in equation (1) for T10. In NAT (Figure 7a), Ω for T10 shows a pronounced upward trend for the entire period, indicating an increasing TC contribution to extreme rain amount. The long-term variation of Ω tracks well the percentage change in the area of the warm pool, suggesting a possible relationship between TC-rain contribution to extreme rain events and the relative size of the warm pool. The positive trends appear to begin in 1984–85, indicating increasing TC contribution to extreme rainfall associated with a substantially expanded warm pool in NAT in the last two decades. By comparison, Ω in WNP (Figure 7b) increases only modestly with large decadal-scale variation. This modest overall increase in TC-rain contribution is consistent with the smaller percentage increase in warm pool size in WNP compared to NAT, during the same periods.

[18] In the following, we provide a summary of the main results and a discussion of possible influences due to inclusion of the pre-SSM/I period. From Table 3, for

NAT, there are positive trends for total TC-rain (24.9 mm/decade). This is a substantial rate approximately equal to 41% per-decade change in the mean. Here, all extreme rain categories (T20, through T5) show significant increase ranging from 14.8 to 7.4 mm/decade, or approximately 57–75% per-decade change in the mean. These trends are highly significant (>99% c.l.) for the entire data period. When data of the pre-SSM/I period are excluded, only the total TC-rain remains significant (>95% c.l.). Here, the trends for TC related T20, T10 and T5 extreme rains remain positive in the 11.3 to 4.8 mm/decade range, which corresponds approximately to 32–34% per-decade change in the mean. The drop in signal using only post-SSM/I data may be due to sampling errors from the shorter record, and/or due to possible influence of data inhomogeneity between the pre- and post-SSM/I periods. Notably, the fractional contribution of TC in extreme rain, Ω , indicates a positive trend in the range of 12–18% per-decade for all extreme rainfall categories, when computed using data for the entire period. Using post-SSM/I data only, the magnitudes of the Ω trends are comparable at a range of 11–15% per-decade. These trends are only marginally significant (>90% c.l.), possibly due to reduced degree of freedom in the shorter data record. The consistent increase of Ω for increasing extreme rain categories for both data periods suggests a minimal impact of data inhomogeneity, because the ratio of extreme rain to total rain may be less sensitive to the different rainfall algorithms used in the GPCP data. With respect to SST, separate computation that Ω has a significant correlation (0.53 for T10) with the size of warm pool which is expanding at 14% per-decade over the entire period. This correlation increases slightly to 0.55 for the post-SSM/I period, when the NAT warm pool is expanding at 22%. Detrending both time series, the correlations are reduced to 0.26 for the entire period, and to 0.41 for the post-SSM/I period, indicating that a significant portion of the correlation between Ω and the warm pool area is contributed by the linear trend.

[19] In WNP, large interannual and decadal oscillation dominate the TC activity with peaks in the mid-1990s which coincide with the first half of the post-SSM/I era (see also Figure 4d). Trend signals computed in WNP are masked by the dominant decadal variation. For example, the positive trends in extreme rain categories computed from the whole data period that range from 26.0 to 15.1 mm/decade for T20 through T5 (Table 3), are likely due to the steep rise in TC activities from the mid-1980s to mid-1990s noted in previous discussions (see Figure 5d). The corresponding change in Ω is approximately constant at 3–4% for all extreme rain categories. For the post-SSM/I period only, the negative and small trend signals for all extreme rain statistics are again most likely related to the negative swing of the decadal variation in TC activities in the WNP since 1995. Notwithstanding the decline in total TC rain and T20_{TC} rain, Ω for T10 and T5 still increases at 3% per-decade in the post-SSM/I period. These trends are however not significant (<95% c.l.), being masked by large interannual and interdecadal variability. Also worth noting is the smaller change of warm pool area in WNP (6% per-decade for the entire period and 9% for the post-SSM/I period), compared to NAT. There are weak negative corre-

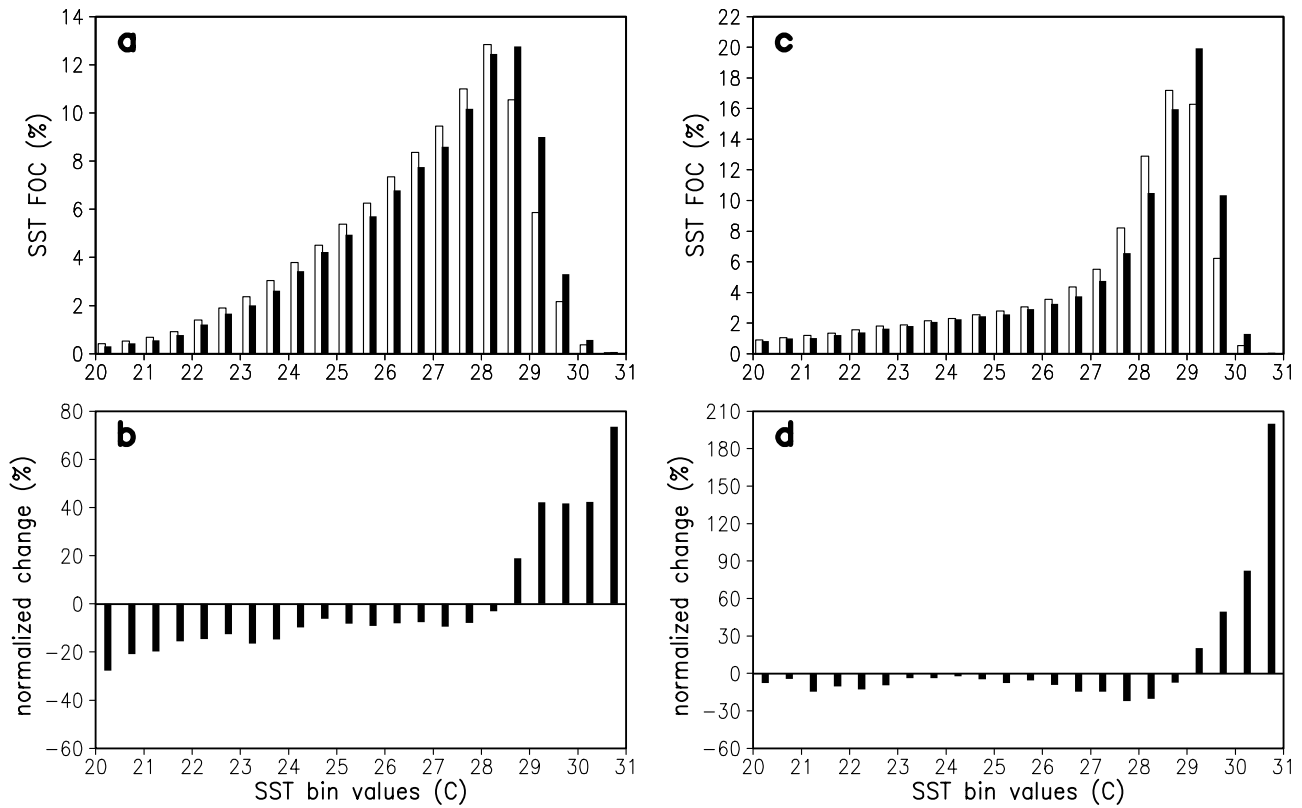


Figure 6. (a) Climatological frequency of occurrence (FOC) of SST binned with 0.5°C interval, during JASON of the first 13 years (1979–1991, outlined bar) and the latter 13 years (1993–2005, filled bar), and (b) shift in FOC shown as the difference between the SST FOC of the latter period (1993–2005) and the first period (1979–1991) normalized by the mean of these two periods, for NAT. (c) and (d), as in (a) and (b), except for WNP.

lations (−0.22) between Ω T10 and the warm pool area for the entire period, and (−0.28) during the post-SSM/I period, both are insignificant at the 95% c.l. Detrending the time series increases the negative correlation to −0.58 (>95%

c.l.) for the entire period, and −0.59 (>95% c.l.) for the post-SSM/I period. The higher correlations after detrending are most likely indicative of the strong control of ENSO and related coupled ocean–atmosphere interactions in WNP. In

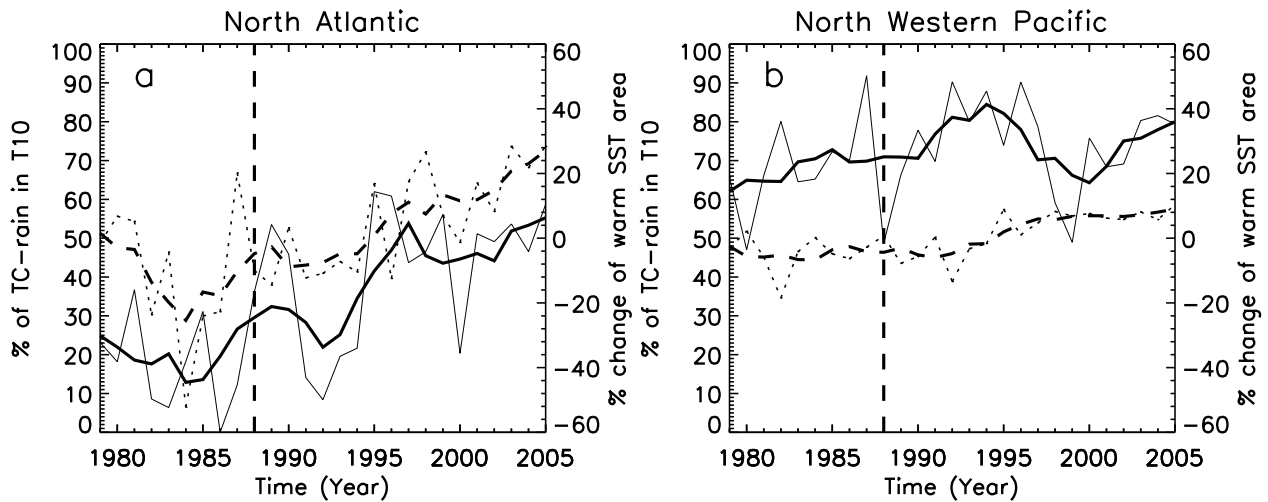


Figure 7. Time variation of ratio of cumulative extreme TC rainfall amount to total rainfall, Ω , in T10 from GPCP (solid line). Dotted line shows the normalized anomaly in percentage of warm pool area (defined as monthly SST > 28°C) over JASON season for each year for (a) NAT and (b) WNP. Thick lines show 5-year running mean. Vertical dash lines separate the pre-SSM/I and post-SSM/I period.

both ocean basins, clearly the linear trend is affected by interannual/interdecadal variability of the warm pool area, especially for WNP, where such variability may have masked any trend signals in the extreme rainfall statistics.

3.4. Comparison With Previous Work

[20] Recently, *Emanuel* [2005] and *Webster et al.* [2005] found nearly doubling of the number of intense TCs (Categories 4 and 5 based on the Saffir–Simpson scale) in both NAT and WNP. However *Klotzbach* [2006] found a much smaller trend of about 10% globally in Categories 4 and 5, and a large increase in Categories 4 and 5 in NAT, but not in WNP. *Kossin et al.* [2007] reported that there are no robust trends in intense TCs in all ocean basins, except for the North Atlantic since 1983. Our results are consistent with these authors in that for most TC rainfall statistics, significant trends are found in NAT, but only mixed signals are found in WNP. The difference in trend signals between the two oceans may be related to the differences in the rate of expansion of the warm pools ($SST > 28^{\circ}\text{C}$), and in the underlying relationship with the atmosphere and warm pool SST. On the basis of the regression of total TC rain and warm pool area, we found that an increase of approximately 13 mm per decade of total TC rain can be expected from the observed expansion rate (14% per decade) of the warm pool in NAT. This means that slightly more than 50% of the observed increased in TC rain (24.9 mm, as shown in Table 3) can be explained by increase in warm pool area in NAT. For the WNP, the relationship between the warm pool area and total TC rain is dominated by the decadal and ENSO variability, and no significant signals in TC total rain can be attributed to SST trend. While we have found increased rainfall contribution by active TC activity associated with the expansion of warm pool in NAT using GPCP data, we cannot address or extrapolate our results for the pre-satellite period, for example, active TC activity in NAT during late 1920s and late 1960s [*Goldenberg et al.*, 2001]. For WNP, the GPCP record length may still be too short to extract significant trend signals.

[21] Our approach differs from previous studies in that we focus on detecting TC extreme rainfall trend signals over the tropical oceans using multi-decadal satellite rainfall data from GPCP. We used a unified classification of rain extremes and TC-rain in both oceans. Hence our definition of TC-rain is not subject to the uncertainties due to secular changes in the definition of TC intensity used by different operational centers. By definition, the contribution of TC-rain to accumulated extreme rain, Ω , is an integral property and a ratio that is a more stable quantity compared to TC intensity defined for individual storms, and is therefore less sensitive to inhomogeneity in GPCP data due to different instruments mix between the pre-SSM/I and post-SSM/I periods. Our results are consistent with recent high-resolution global modeling experiments indicating increase in number of simulated high-intensity TCs under warmer SST and higher specific humidity conditions [*Bengtsson et al.*, 2007]. The increase in hurricane rainfall and rainfall intensity in NAT is also consistent with the modeling study of *Knutson and Tuleya* [2004], and observational study of *Lonfat et al.* [2004]

where they showed increasing rain rates with increasing tropical cyclone intensity.

4. Conclusions

[22] Using TRMM and GPCP data, we have documented the mean and long-term changes in the contribution of TCs to rainfall as a function of rain rates in NAT, and WNP. We find that during the TC season, July–November, TC accounts for approximately 8% of the total rain events, but about 17% of the rainfall amount in NAT, as compared to 9% of rain events and 21% of rainfall amount in WNP based on TRMM data from 1998 to 2005. Overall, TCs in WNP appear to be more energetic than NAT in terms of having higher average rainfall intensity, and higher rainfall thresholds for given percentile extreme rain rates. Using the full record (1979–2005) GPCP data, we find a substantial shift in the rainfall PDF during the TC season, manifested as an increase in extreme rain amount and events in both oceans. However, with regard to the relationships between TCs and extreme rain, substantial differences are found between the two ocean domains, especially when the pre-SSM/I data are excluded. In NAT, the contributions of TC to the top extreme rainfall are increasing at 12–18% per-decade, and at a comparable rate of 11–15% per-decade for post-SSM/I period. In contrast, WNP TCs only contribute to a modest increase of about 3–4% per-decade in extreme rain. Our results suggest that TCs are contributing increasingly more in rainfall extreme events in the past two decades in NAT. However, in WNP, the trend signals are mixed because of the larger influences of interannual and decadal variations and possibly inhomogeneity in the GPCP data. We speculate that the different rate of increase may be related to the larger percentage increase in the size of the warm pool in NAT compared to WNP, as well as to the large-scale circulation and moisture conditions pertaining to each ocean basin. This is consistent with a recent study [*Vecchi and Soden*, 2007] which suggests that tropical cyclone potential intensity is more sensitive to localized SST changes stemming from coupled ocean-atmosphere dynamical feedback, than to the uniform SST pattern associated with greenhouse-gas induced warming.

[23] Obviously, the results in this work are subject to uncertainties in the satellite rainfall data. We have shown that the temporal inhomogeneity in GPCP data from the pre-SSM/I and post-SSM/I period may affect some of the derived trends. Our study suggests that useful climate signals could be detected for extreme rainfall statistics from the GPCP data. It also demonstrates the need for realistic error estimates with respect to data inhomogeneity in multi-decadal global satellite data, and cross-validation with model results. Finally, our results are consistent with the notion that regional climate change signals tend to manifest themselves in statistics of extreme events, rather than in changes in the mean. Efforts are now underway to extend this study to other ocean basins and to examine different parts of the spectrum and their relationship to rainfall characteristics and associated weather phenomena and climate processes. These efforts underscore the need for extending and improving long-term rainfall data sets to

obtain reliable estimates of rainfall PDFs, such as those anticipated by the Global Precipitation Measurement (GPM) program [Smith et al., 2007]. The continuation of TRMM data into the GPM era, and the continuously reprocessing of satellite data are critical for quantitative assessment of the role of rainfall on the atmospheric water cycle associated with climate change.

[24] **Acknowledgments.** This work is supported by the Precipitation Measuring Mission (Headquarter Manager: Dr. R. Kakar), NASA Earth Science Division. We thank Dr. Chris Landsea and two anonymous reviewers for constructive comments that have improved the manuscript.

References

- Adler, R. F., et al. (2003), The version-2 Global Precipitation Climatology Project (GPCP) monthly precipitation analysis (1979–present), *J. Hydrometeorol.*, *4*, 1147–1167.
- Bengtsson, L., K. I. Hodges, M. Esch, N. Keenlyside, L. Kornbluh, J. J. Luo, and T. Yamagata (2007), How may tropical cyclone change in a warmer climate?, *Tellus*, *59*, 539–561.
- Chan, J. C. L., and J. E. Shi (1996), Long-term trends and interannual variability in tropical cyclone activity over the western North Pacific, *Geophys. Res. Lett.*, *23*, 2765–2767.
- Chan, J. C. L., and K. S. Liu (2004), Global warming and western North Pacific typhoon activity from an observational perspective, *J. Clim.*, *17*, 4590–4602.
- Chu, J.-H., C. R. Sampson, A. S. Levine, and E. Fukada (2002), The Joint Typhoon Warning Center Tropical Cyclone Best-Tracks, 1945–2000. NRL Ref. Num.: NRL/MR/7540-02-16. (Available at http://metocph.nmci.navy.mil/jtwc/best_tracks/TC_bt_report.html)
- Dutton, J. F., C. J. Poulsen, and J. L. Evans (2000), The effect of global climate change on the regions of tropical convection in CSM1, *Geophys. Res. Lett.*, *27*, 3049–3052.
- Emanuel, K. A. (1987), The dependence of hurricane intensity on climate, *Nature*, *326*, 483–485.
- Emanuel, K. (2005), Increasing destructiveness of tropical cyclones over the past 30 years, *Nature*, *436*, 686–688.
- Goldenberg, S. B., and L. J. Shapiro (1996), Physical mechanisms for the association of El Niño and West African rainfall with Atlantic major hurricane activity, *J. Clim.*, *9*, 1169–1187.
- Goldenberg, S. B., C. Landsea, A. M. Mestas-Núñez, and W. M. Gray (2001), The recent increase in Atlantic hurricane activity, *Science*, *293*, 474–479.
- Gray, W. M. (1968), Global view of the origin of tropical disturbances and storms, *Mon. Weather Rev.*, *96*, 669–700.
- Gray, W. M. (1984), Atlantic seasonal hurricane frequency. part I: El Niño and 30 mb quasi-biennial oscillation influences, *Mon. Weather Rev.*, *112*, 1649–1668.
- Gray, W. M. (1990), Strong association between West African rainfall and U.S. landfall of intense hurricanes, *Science*, *249*, 1251–1256.
- Groisman, P. Y., et al. (2004), Contemporary changes of the hydrological cycle over the contiguous United States: Trenes derived from in situ observations, *J. Hydrometeorol.*, *5*, 64–85.
- Henderson-Sellers, A., et al. (1998), Tropical cyclones and global climate change: A post-IPCC assessment, *Bull. Am. Meteorol. Soc.*, *79*, 19–38.
- Huffman, G., R. F. Adler, D. T. Bolvin, G. Gu, E. J. Nelkin, K. P. Bowman, Y. Hong, E. F. Stocker, and D. B. Wolff (2007), The TRMM multisatellite precipitation analysis (TMPA): Quasi-global, multiyear, combined-sensor precipitation estimates at fine scales, *J. Hydrometeorol.*, *8*, 38–55.
- Jarvinen, B. R., C. J. Neumann, and M. A. S. Davis (1984), A tropical cyclone data tape for the North Atlantic Basin, 1886–1983: Contents, limitations, and uses. NOAA Technical Memorandum NWS NHC 22, Coral Gables, Fla., 21 pp. (Available at <http://www.nhc.noaa.gov/pdf/NWS-NHC-1988-22.pdf>)
- Karl, T. R., and R. W. Knight (1998), Secular trends of precipitation amount, frequency, and intensity in the United States, *Bull. Am. Meteorol. Soc.*, *79*, 231–241.
- Klotzbach, P. J. (2006), Trends in global tropical cyclone activity over the past twenty years (1986–2005), *Geophys. Res. Lett.*, *33*, L10805, doi:10.1029/2006GL025881.
- Knaff, J. A. (1997), Implications of summertime sea level pressure anomalies in the tropical Atlantic region, *J. Clim.*, *10*, 789–804.
- Knutson, T. R., and R. E. Tuleya (2004), Impact of CO₂-induced warming on simulated hurricane intensity and precipitation: Sensitivity to the choice of climate model and convective parameterization, *J. Clim.*, *17*, 3477–3495.
- Kossin, J. P., K. R. Knapp, D. J. Vimont, R. J. Murnane, and B. A. Harper (2007), A globally consistent reanalysis of hurricane variability and trends, *Geophys. Res. Lett.*, *34*, L04815, doi:10.1029/2006GL028836.
- Landsea, C. W. (1993), A climatology of intense (or major) Atlantic hurricanes, *Mon. Weather Rev.*, *121*, 1703–1713.
- Landsea, C. W., and W. M. Gray (1992), The strong association between Western Sahel monsoon rainfall and intense Atlantic hurricanes, *J. Clim.*, *5*, 435–453.
- Landsea, C. W., W. M. Gray, P. W. Mielke Jr., and K. J. Berry (1994), Seasonal forecasting of Atlantic hurricane activity, *Weather*, *49*, 273–283.
- Landsea, C. W., G. D. Bell, W. M. Gray, and S. B. Goldenberg (1998), The extremely active 1995 Atlantic hurricane season: Environmental conditions and verification of seasonal forecasts, *Mon. Weather Rev.*, *126*, 1174–1193.
- Landsea, C. W., B. A. Harper, K. Hoarau, and J. A. Knaff (2006), Can we detect trends in extreme tropical cyclones?, *Science*, *313*, 452–454.
- Larson, J., Y. Zhou, and R. W. Higgins (2005), Characteristics of land-falling tropical cyclones in the United States and Mexico: Climatology and interannual variability, *J. Clim.*, *18*, 1247–1262.
- Lau, K. M., and H. T. Wu (2007), Detecting trends in tropical rainfall characteristics, 1979–2003, *Int. J. Climatol.*, *27*, 979–988.
- Lonfat, M., F. D. Marks Jr., and S. S. Chen (2004), Precipitation distribution in tropical cyclones using the Tropical Rainfall Measuring Mission (TRMM) microwave imager: A global perspective, *Mon. Weather Rev.*, *132*, 1645–1660.
- Pielke, R. A., Jr., C. Landsea, M. Mayfield, J. Laver, and R. Pasch (2005), Hurricanes and global warming, *Bull. Am. Meteorol. Soc.*, *86*, 1571–1575.
- Rayner, N. A., D. E. Parker, E. B. Horton, C. K. Folland, L. V. Alexander, D. P. Rowell, E. C. Kent, and A. Kaplan (2003), Global analyses of SST, sea ice and night marine air temperature since the late nineteenth century, *J. Geophys. Res.*, *108*(D14), 4407, doi:10.1029/2002JD002670.
- Rodgers, E. B., R. F. Adler, and H. F. Pierce (2000), Contribution of tropical cyclones to the North Pacific climatological rainfall as observed from satellites, *J. Appl. Meteorol.*, *39*, 1658–1678.
- Rodgers, E. B., R. F. Adler, and H. F. Pierce (2001), Contribution of tropical cyclones to the North Atlantic climatological rainfall as observed from satellites, *J. Appl. Meteorol.*, *40*, 1785–1800.
- Saunders, M. A., and A. R. Harris (1997), Statistical evidence links exceptional 1995 Atlantic hurricane season to record sea warming, *Geophys. Res. Lett.*, *24*, 1255–1258.
- Shapiro, L. J. (1982), Hurricane climatic fluctuations. part II: Relation to large-scale circulation, *Mon. Weather Rev.*, *110*, 1014–1023.
- Shapiro, L. J. (1987), Month-to-month variability of the Atlantic tropical circulation and its relationship to tropical storm formation, *Mon. Weather Rev.*, *115*, 2598–2614.
- Shapiro, L. J. (1989), The relationship of the quasi-biennial oscillation to Atlantic tropical storm activity, *Mon. Weather Rev.*, *117*, 2598–2614.
- Shapiro, L. J., and S. B. Goldenberg (1998), Atlantic sea surface temperatures and tropical cyclone formation, *J. Clim.*, *11*, 578–590.
- Shepherd, J. M., and T. Knutson (2006), The current debate on the linkage between global warming and hurricanes, *Geogr. Compass*, *1*(1), 1–24, doi:10.1111/j.1749-8198.2006.00002.x.
- Shepherd, J. M., A. Grundstein, and T. L. Mote (2007), Quantifying the contribution of tropical cyclones to extreme rainfall along the coastal southeastern United States, *Geophys. Res. Lett.*, *34*, L23810, doi:10.1029/2007GL031694.
- Smith, E. A., et al. (2007), International Global Precipitation Measurement (GPM) program and mission: An overview, in *Measuring Precipitation From Space: EURAINSAT and the Future*, edited by V. Levizzani, P. Bauer, and F. J. Turk, pp. 611–653, Springer, Netherlands.
- Trenberth, K. (2005), Uncertainty in hurricanes and global warming, *Science*, *308*, 1753–1754.
- Trenberth, K. E., et al. (2007), Observations: Surface and Atmospheric Climate Change, in *Climate Change 2007: The Physical Science Basis. Contribution of Working Group I to the Fourth Assessment Report of the Intergovernmental Panel on Climate Change*, edited by S. Solomon et al., Cambridge Univ. Press, Cambridge, U.K. and New York, N.Y.
- Trenberth, K. E., A. Dai, R. M. Rasmussen, and D. B. Parsons (2003), The changing character of precipitation, *Bull. Am. Meteorol. Soc.*, *84*, 1205–1217.
- Vecchi, G. A., and B. J. Soden (2007), Effect of remote sea surface temperature change on tropical cyclone potential intensity, *Nature*, *450*, 1066–1070.
- Velden, C., et al. (2006), The Dvorak tropical cyclone intensity estimation technique: A satellite-based method that has endured for over 30 years, *Bull. Am. Meteorol. Soc.*, *87*, 1195–1210.

- Wang, B., and J. C. L. Chan (2002), How strong ENSO events affect tropical storm activity over the western North Pacific, *J. Clim.*, *15*, 1643–1658.
- Wang, C. Z., D. B. Enfield, S. K. Lee, and C. W. Landsea (2006), Influences of the Atlantic warm pool on western hemisphere summer rainfall and Atlantic hurricanes, *J. Clim.*, *19*, 3011–3028.
- Wang, C. S., K. Lee, and D. B. Enfield (2008), Climate response to anomalously larger and small Atlantic warm pools during the summer, *J. Clim.*, *21*, 2437–2450.
- Webster, P. J., G. J. Holland, J. A. Curry, and H.-R. Chang (2005), Changes in tropical cyclone number, duration, and intensity in a warming environment, *Science*, *309*, 1844–1846.
- Wilks, D. S. (1995), *Statistic Methods in the Atmospheric Sciences*, pp. 160–176, Academic, New York.
- Wu, Y., S. Wu, and P. Zhai (2007), The impact of tropical cyclones on Hainan Island's extreme and total precipitation, *Int. J. Climatol.*, *27*, 1059–1064.
- Xie, P., J. E. Janowiak, P. A. Arkin, R. F. Adler, A. Gruber, R. Ferraro, G. J. Huffman, and S. Curtis (2003), GPCP pentad precipitation analyses: An experimental dataset based on gauge observations and satellite estimates, *J. Clim.*, *16*, 2197–2214.

K.-M. Lau, Laboratory for Atmospheres, Code 613, NASA, Goddard Space Flight Center, Greenbelt, MD 20771, USA. (william.k.lau@nasa.gov)

H.-T. Wu and Y. P. Zhou, Climate and Radiation Branch, Code 613.2, NASA, Goddard Space Flight Center, Greenbelt, MD 20771, USA. (huey-tzu.wu-1@mail.nasa.gov; yaping.zhou-1@nasa.gov)